Modeling of the Electrostatic Interaction of Ions in Dry, Isolated Micelles of AOT by the Method of Direct Optimization

A. I. Bulavchenko,*,† A. F. Batishchev,‡ E. K. Batishcheva,† and V. G. Torgov†

Institute of Inorganic Chemistry and Institute of Mathematics, Siberian Branch of the Russian Academy of Sciences, Novosibirsk, Russia

Received: December 4, 2001

A simple model of a dry reversed micelle of ionic surfactants is proposed, according to which during the optimization procedures the ions move over certain closed surfaces in a vacuum at $T = 0$ K .The electrostatic interactions of discrete ions in dry, reversed micelles of AOT are calculated as a function of the sizes of the ions, ion charges, and the optimum positions of the ions in the polar cavity of the micelles. It is shown that when the counterions penetrate the layer of the potential-determining ions, the electrostatic interaction begins to favor the self-organization of the ionic surfactants over that of the reversed micelles. The distribution of the electrostatic potential in the polar cavity of micelles of different shapes (a sphere, a spheroid, a prolate ellipsoid) is calculated. In the models in which the charge is taken to be discrete, the electrostatic field extends beyond the double electric layer (DEL); the sign of the potential coincides with that of the counterion. It is shown that in the analysis of structures of dry, reversed micelles the possibility of the formation of voids (in the surface layer of polar groups and in the center) as well as the density of packing should be taken into account by using a specially developed approach. The most probable structural parameters of AOT micelles are determined for different counterions (Li^+, Na^+, Cs^+, $[Co(H_2O)_6]^{2+}$, La^{3+}).

1. Introduction

Recently, there has been renewed interest in micelles formed by surfactants. Although the first "wave" of interest was mainly due to the ability of microemulsions to drastically increase oil recovery from complex oil pools,[1] the recent interest was undoubtedly caused by the progress in the supramolecular chemistry and nanotechnology.[2] The structure of micellar solutions (the presence of mobile nanocavities of a high polarity) allows various physicochemical interactions to be performed in micelles on a qualitatively different level of structural organization. Thus, in reversed micelles, it was possible to obtain nanoparticles of a preset size and shape.[3−5] Micellar solutions and microemulsions have been employed to separate and concentrate metals[6−8] and biomolecules[9−11] and to control many chemical reactions kinetically.[12−14] In all these studies, the fine structure, size, and shape of the micelles were the determining parameters of micelles as "molecular" reactors,[15,16] and it is these parameters that determined the success of the interactions.

Most of the experimental studies used sodium bis(2-ethylhexyl)sulfosuccinate (NaAOT), an ionic oil-soluble surfactant, for the formation of micelles. The presence of strong electrostatic fields in the NaAOT micelles that were due to the presence of spatially separated charges (double electric layer, DEL) had a substantial influence on the conditions of physicochemical interactions.[17] Therefore, the structure of DEL in reversed micelles and the effect of DEL on the micelle formation thermodynamics and structural transitions have been studied in a series of theoretical works. A model of DEL has been proposed, and the distribution of the potential in the micellar aqueous core has been studied.[18] It was found that as a result of the counterions in the inner layer coming close to each other because of the greater curvature of this layer there is an increase in the free energy and the DEL effect begins to be comparable with the steric effects of hydrocarbon chains. The results of theoretical and experiment studies indicated[20] that the electrostatic interaction of ions has a substantial effect on the size and shape of micelles. In the examples cited above, the DEL was described by the Poisson−Boltzmann equation with different levels of approximations and assumptions. The charge of the potential-determining ions in the micelle was taken to be uniformly "smeared " over the micellar surface (or within a thin layer[21]) whereas the counterions formed an inner, diffused plate and did not interact with each other (the Gouy−Chapman model of DEL[22]). For a qualitative evaluation of the electrostatic interactions, the simplest equations for the energy of capacitors of different shapes with parallel plates were used.[23] The sizes of the ions were not taken into account.

Measurements of the hydrodynamic radius and the radius of gyration indicated, however, that "dry" micelles of NaAOT have low numbers of aggregation[24,25] and hence contain an inconsiderable number of ions. It was also found that mixed micelles formed by ionic and nonionic surfactants[26] may contain several ions. In the absence of water (or other polar additives), it seems unlikely that the ion pairs will dissociate, so the use of "diffuse" models for dry micelles is not quite justified.

In refs 27−29, the structure of dry micelles of sodium bis-(2-ethylhexyl)- phosphate (the NaDEHP molecule is structurally related to NaAOT) was studied using a new approach in which the reversed micelles of ionic surfactants at low water content are treated as ionic crystallites. According to the authors' opinion, the electrostatic interactions between the ions in the NaDEHP molecules are responsible for the formation of "giant" rodlike crystallites. With the addition of water, the numbers of

* Corresponding author. E-mail: bulavch@che.nsk.su.
† Institute of Inorganic Chemistry, Siberian Branch of the Russian Academy of Sciences.
‡ Institute of Mathematics, Siberian Branch of the Russian Academy of Sciences.

10.1021/jp0144000 CCC: $22.00
Published on Web 06/04/2002

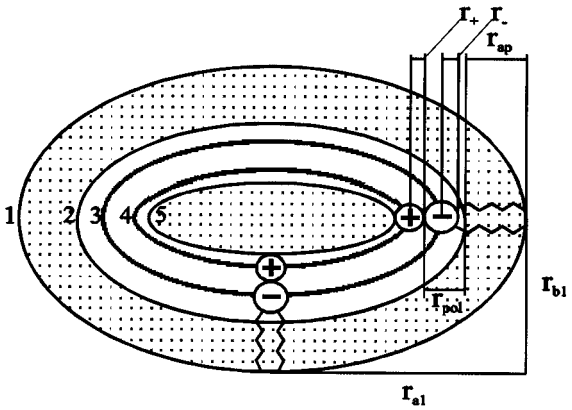

Figure 1. Schematic presentation of the model of the reversed micelle of AOT for structure optimization analysis. Explanations are given in the text.

aggregation decrease, and the crystallites are transformed into reversed micelles.

Here we present a structural analysis of dry, reversed micelles of AOT with different counterions performed by calculating and optimizing the Coulomb interaction between ions in micelles of different shapes and with different numbers of aggregation.

2. Description of the Models and the Methods of Numerical Simulation

Interacting Surfaces. The fine structure of reversed micelles is, to a large extent, determined by the structure of the surfactants from which they are formed (the length of the hydrophobic part of the surfactant molecule and the parameters of the hydrophilic "head"). Generally, three geometries are used to describe the micellar shape: a sphere and a prolate and an oblate ellipsoid.[30] The outer surface 1 separating the micelle from the solvent extends over the ends of the hydrocarbon "tails" of the surfactant molecules (Figure 1). Corresponding to this surface is the hydrodynamic radius of the micelle, which is calculated from the large (r_{a1}) and small (r_{b1}) half-axes of this surface by the equations given in ref 31. The polar part of the micelle is separated from the nonpolar part by surface 2. The parameters of this surface are given by

$$r_{a2} = r_{a1} - r_{ap}$$
$$r_{b2} = r_{b1} - r_{ap}$$

where r_{ap} is the length of the hydrocarbon tail of the surfactant molecule. This surface was used to calculate the volume and surface area of the polar part (cavity) of the micelle.

The interaction between the ions takes place in the polar part of the micelle. Let the potential-determining ions lie on surface 3 with the parameters

$$r_{a3} = r_{a2} - r_{pol} + r_{-}$$
$$r_{b3} = r_{b2} - r_{pol} + r_{-}$$

where r_{pol} is the length of the polar part of the molecule without a counterion and r_{-} is the radius of the potential-determining ion. The layer of the counterions forms surface 4, which is equidistant from surface 3. The maximum distance between surfaces 3 and 4 is determined by the sum of the radii of the potential-determining ion and the counterion. At zero distance, all ions lie on surface 3. The minimum distance between surfaces 2 and 4 is determined by the radius of the counterion. Finally, surface 5 is introduced to calculate the volume and area of the central cavity, which has no ions (in Figure 1, the cavities without ions are shaded). It should be noted that surfaces 2, 3, and 5 follow the shape of the external surface 1. Thus, in a spheroidal micelle, surfaces 2, 3, and 5 will be spheroidal, etc., but surface 4 is not spheroidal and is described by higher-order equations.

Parameters of the Surfactants. The following parameters of AOT were used in the calculations. The length of the nonpolar part of the molecule (r_{ap}) was taken to be equal to 0.7 nm, and that of the polar part (r_{pol}), to 0.5 nm. The area per molecule in the flat surface layer (S_{org}) was assigned the value of 0.63 nm^2 (in different works, these values range from 0.4 to 0.7 nm^2 [32,33]). The surfactant molecule was modeled by two active centers, a potential-determinig ion, and a counterion. The negative potential-determining charge of AOT appears to be delocalized on the three oxygens of the sulfo group and therefore was modeled by a spherical ion of charge -1 residing in the center of a sphere of radius 0.2 nm. The radii of Li^+, Na^+, Cs^+, and La^{3+} were taken from[34] the radius that $Co(H_2O)_6^{2+}$ was taken from.[20]

The numbers of aggregation of the micelles, N_{ag}, were calculated by dividing the area S_2 by S_{org}. According to the geometrical approach,[31] it was assumed that the surfactant aggregation to micelles takes place at a constant area (S_{org}) per surfactant molecule in a flat surface layer.

It should be noted that in ref 35 the value of r_{-} was taken to be equal to 0.3 nm. We think that this is an overestimated value because, as will be shown later, the use of this value for spherical micelles leads to large numbers of aggregation and the calculated hydrodynamic radius exceeds the experimental value. The same authors used surface 3 for the calculation of the area occupied per surfactant molecule at the interface, not surface 2 as used in this work. In our opinion, it is preferable to use surface 2 as the dividing surface. In this case, the use of experimental data for S_{org} derived from measurements of the interface tension on the macroscopic water/oil interfaces is better justified.

Interaction Potential. The energy of the system is obtained by summing the interactions of all the ions with each other according to the "each with each" principle (the atom−atom approximation):

$$U = \sum_i \sum_j U_{ij}$$

At this stage of investigation in our work, we took into account only the Coulomb potential and the positive part of the Lennard-Jones potential

$$U_{ij} = E_{Cul} + U^{+}_{L-D} = -\frac{q_i q_j}{4\pi\epsilon_0\epsilon_{ij} r_{ij}} + \frac{A_{ij}}{r_{ij}^{12}}$$

where q_i and q_j are the charges of the interacting ions, r_{ij} is the distance between them, ϵ_{ij} is the dielectric permeability, ϵ_o is the electrostatic constant, and A_{ij} is the Lennard-Jones constant.

To estimate the contributions of the interactions of counterions and potential-determining ions with and between each other, the overall Coulomb interaction was broken into components:

$$E_{Cul} = E_{++} + E_{--} + E_{+-}$$

In the calculations of the Coulomb interactions in dry micelles, ϵ_{ij} was taken to be equal to unity. Index i refers to the potential-determining ions, and j, to the counterions. The constant of the Lennard-Jones potential, A_{ij}, depends only on the size and charge of the interacting ions and was chosen so

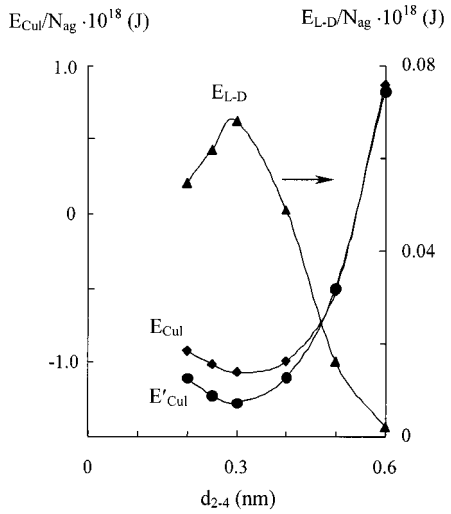

Figure 2. Change in the electrostatic and Lennard-Jones interactions when Na^+ penetrates the layer of the potential-determining ions of a spherical micelle of NaAOT ($N_{ag} = 14$). At $d_{2-4} = 0.6$ nm, the Na^+ ions are at the maximum possible distance from the potential-determining ions. At $d_{2-4} = 0.3$ nm, the Na^+ ions are on one surface 3. The dependence of E_{CuI} was obtained with the account of only the positive part of the Lennard-Jones potential. For E_{CuI}', the full potential was taken into account.

that the minimum of the U_{ij} dependence on r_{ij} for the opposite charges was at the distance equal to the sum of their ionic radii.

The positive part of the Lennard-Jones interaction (U^+_{L-D}) was introduced to prevent the "penetration" of ions into each other and thus to take into account the sizes of the ions. This interaction was taken into account only when the distance between surfaces 3 and 4 was less than the sum of the radii of the counterion and the potential-determining ion. In this case, the Lennard-Jones interaction was taken into account in the optimization procedures but was not included in the final values of U_{ij} because of its inconsiderable size.

A similar way to calculate A_{ij} has been used when determining the energy of the crystal lattice of ionic crystals.[34]

To evaluate the effects of the employed approximations, the energy of a spherical micelle of NaAOT was calculated using the "full" Lennard-Jones potential (Figure 2). The Lennard-Jones parameters for the calculation of the interactions between the ions were taken from ref 35. As follows from Figure 2, the contribution of the Lennard-Jones interaction is at its maximum when all ions are on one surface, and in this case, the contribution amounts to no more than 8% of the Coulomb interaction. But the Lennard-Jones interaction of ions leads to a 20% increase (modulo) of the electrostatic interaction. This increase of the Coulomb attraction is due to the fact that the van der Waals attraction between the potential-determining ions and counterions bring them still closer to each other. Because for many ions the literature gives no Lennard-Jones parameters and the available values had been chosen rather arbitrarily and have an empirical character, at this stage of the investigations, we decided to restrict ourselves to the positive component of the Lennard-Jones potential.

Optimization Procedures. The optimization problem reduces to placing the potential-determining ions and counterions onto surfaces 3 and 4, respectively, to obtain the minimum energy of the electrostatic interaction of all the ions with each other (it was assumed that $T = 0$ K). This problem was solved within the framework of the direct optimization approach using the conjugated gradients method. In the initial state of the system, the ions occupied random positions on surfaces 3 and 4 (all ions being placed onto the surfaces simultaneously).

With this approach, the effect of the counterions on the final localization of the potential-determining ions was also taken into account during the optimization procedure. This effect was especially pronounced at small values of d_{3-4} and led to a change of the configuration of the potential-determining ions relative to that calculated in the absence of the counterions. It should be noted that in ref 35 the construction of the inner cavity of the micelle was done in steps. First, the positions of the potential-determining ions on the sphere were optimized and fixed, and only then were the counterions introduced into the cavity volume. Therefore, the lateral displacements of the surfactant molecules in the micelle and the effect of the counterions on their localization were not taken into account. Further in our calculations, the counterions were placed directly onto surface 4. Special calculations have shown that the results obtained when ions were introduced into the cavity confined by surface 4 are practically the same as in the case when the ions were placed directly onto the surface.

The program was implemented in Win32 API, and the calculations were performed on a personal computer with a Pentium-3 processor.

To estimate the errors in the optimization procedures, 10 parallel measurements of the Coulomb interaction for micelles were performed. For example, for spherical micelles with $N_{ag} = 14$ and $d_{3-4} = 0$ nm, the mean square error was equal to 7.5×10^{-20} J for the mean value $E_{CuI} = -1.775 \times 10^{-17}$ J.

3. Results and Discussion

3.1. Comparison with the Spherical Capacitor Model. First, it was of interest to compare the calculations obtained with our models in which the energy was obtained by summing the interactions of the point charges with those using the spherical capacitor model in which the charge was treated as being "uniformly" distributed over each of the capacitor plates. For the latter case, the electrostatic interaction gives the following simple expression

$$E^{C}_{CuI} = \frac{q^2}{8\pi\,\epsilon_0\epsilon}\left(\frac{1}{r_3 - d_{3-4}} - \frac{1}{r_3}\right) \qquad (1)$$

where q is the charge on each of the plates. Using eq 1, the values of the electrostatic energy for two capacitors with different values of r_3 at $q = q_e$ were obtained. The summation of the energy of the point charges was calculated by the following equation:

$$E_{CuI} = \sum_i \sum_j \frac{q_i q_j}{4\pi\epsilon_0\epsilon r_{ij}} \qquad (2)$$

The initial value of E_{CuI} was obtained at $i = j = 1$, $q_i = q_j = q_e$, $r_{ij} = 0$, 5 nm (i.e., E_{CuI} was actually equal to the energy of the ion pair). Then the unit charge on each surface was broken into fragments under the observation of the following conditions:

$$|q_i| = |q_j| = |q_e|/N \qquad \text{and} \qquad \sum_i^N |q_i| = \sum_j^N |q_j| = |q_e|$$

Here N is the number of charges on each plate. The calculated dependences are shown in Figure 3. Shown by the dashed line are the values calculated for the capacitors. Plotted on the x axis is the minimal distance between the charges on surface 3

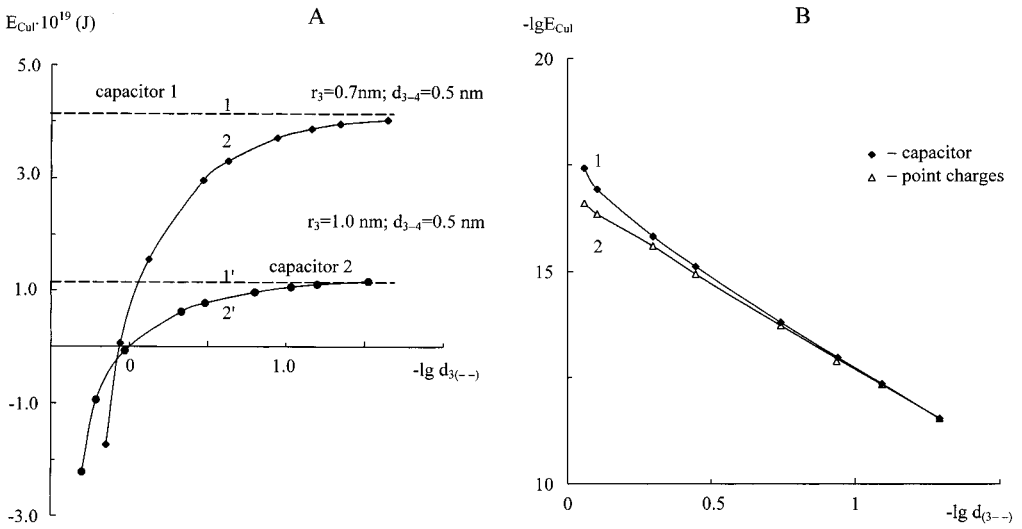

Figure 3. Comparison of the energy of a spherical capacitor with the charges uniformly distributed in the plates (1,1′) with the energy calculated by summing the interactions of the point charges (2,2′). (A) Calculation at a constant overall charge (q_e). (B) Calculation at increasing charge ($r_3 = 1$ nm, $d_{3-4} = 0.5$ nm).

(d_{3--}). This distance was calculated as the average of the distances between the charge and the four nearest neighbors. The mean minimal distances were calculated for each charge, and the values were averaged. As follows from the results shown in Figure 3, the energies calculated for the point charges by eq 2 approach the value obtained by eq 1 only at $d_{3--} \rightarrow \sim 10^{-2}$ nm. These are very small distances, and they did not occur in real micellar systems. It should also be noted that at larger values of d_{3--} the values of E_{Cul} obtained with different models may differ in sign, which indicates that the models with the "uniformly" distributed charge are, in this case, very rough and inaccurate. In passing, an interesting observation should be mentioned: the charge may be considered to be uniformly distributed (i.e., when one can start using the integral eq 1 instead of the sums) only when the distances between the charges are on the order of $\sim 10^{-2}$ nm (for $r_3 \approx 1$ nm and $d_{3-4} \approx 0.5$ nm). Note that the number of charges on each surface approached 10^4 and that the values of each charge approached $|q_e|/10^4$. A similar result was obtained for an increasing charge; here the electrostatic energy was calculated not by "breaking" the unit charge but by the sequential addition of unit charges on the surface (Figure 3B). Unfortunately, a sharp change of the electrostatic energy impelled us to use the logarithmic dependence on which the small differences are poorly discernible.

3.2. Electrostatic Energy of NaAOT Micelles at Different Numbers of Aggregation. The next aim of our numerical simulations was to find the optimum size and shape of reversed micelles of NaAOT by optimizing the Coulomb interaction. To achieve this goal, E_{Cul} must be calculated within a rather wide range of aggregation numbers beginning from the lowest possible values. In addition, the previous calculations have shown that, apart from the size and shape of micelles, the localization of counterions should also be taken into account. In analogous calculations, the so-called "1-D" growth of micelles is usually used when the larger numbers of aggregation are achieved by increasing the large half-axis (r_{a1}) while the small half-axis (r_{b1}) remains constant. Taking into account the sizes of the ions has led to a new problem: the necessity to account for and minimize the volume of voids that appear in micelles with increasing micellar size. There are two types of voids: those forming between surfaces 2 and 5 (i.e., in the layer of the polar groups and DEL) and those in the center of the polar part of the micelle confined by surface 5 (see Figure 1). Such a classification makes sense because the formation of voids of the second type is accompanied by the appearance of a new nanosurface requiring a certain amount of work in its formation.[23] Quantitative evaluation of this work will be done below using the values of S_5 obtained for the calculated micellar structures.

The voids in the structures being formed were taken into account as follows. For each number of aggregation within a given shape, the total volume of voids, V_v, per surfactant molecule in the micelle was calculated:

$$V_v = \frac{V_2 - \sum_j^{N_{ag}} V_j - \sum_i^{N_{ag}/z_i} V_i - \sum_j^{N_{ag}} V_{pol}}{N_{ag}}$$

Here V_2 is the volume of the cavity confined by surface 2, V_j and V_i are the volumes of the potential-determining ion and counterion, respectively, z_i is the charge of the counterion, and V_{pol} is the volume of the polar part of the AOT molecule that has no charge.

Then the parameters (r_{a1}) and (r_{b1}) were varied so as to minimize the values of V_v. As a result, in our case, the growth of micelles with increasing numbers of aggregation was no longer 1-D because r_{b1} was not constant. The minimization of the volume of voids when the counterions penetrated the layer of the potential-determining ions (Figure 4) was done analogously. The calculated values are shown in Figure 5.

From these values, it follows that within one shape (Figure 5A) the decrease in d_{3-4} (i.e., the penetration of counterions into the layer of the potential-determining ions) leads to considerable changes in the energy of electrostatic interaction up to the change of the sign. These changes are especially appreciable in the region of small aggregation numbers. At $d_{3-4} \neq 0$, the most preferable shape is a spheroid followed by a sphere and an elongated ellipsoid (Figure 5B). At low values of d_{3-4}, none of the shapes is preferable.

Distribution of the Potential within the NaAOT Micelle. Figure 6 shows the distribution of the electrostatic potential within spherical micelles of NaAOT. At $d_{3-4} \neq 0$, the potential inside the micelle is positive and nonzero and is dependent on

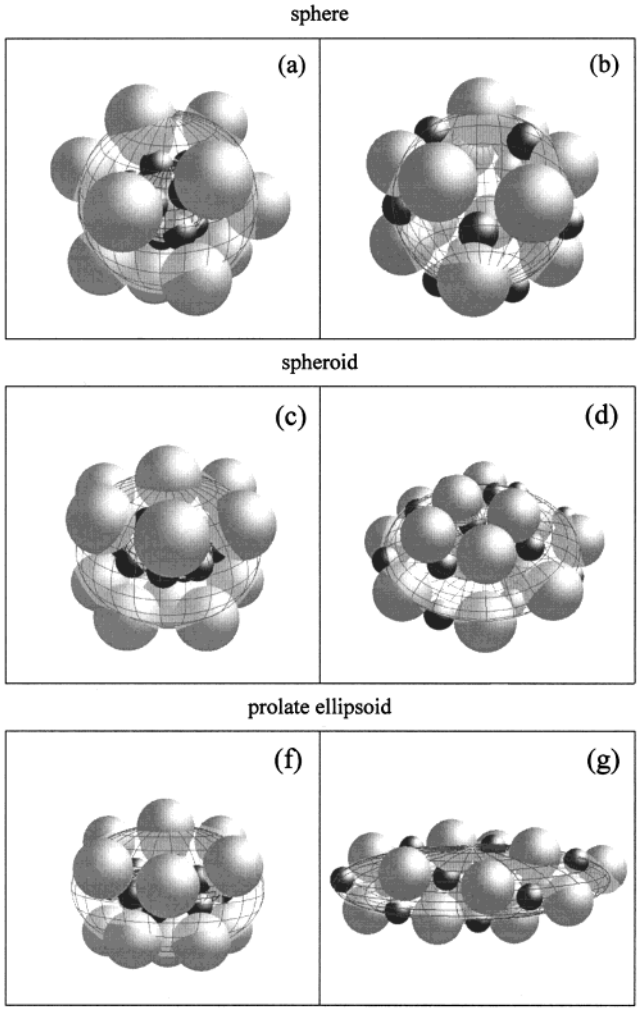

Figure 4. Changes in the structure of NaAOT micelles when the Na^+ ions penetrate the layer of the potential-determining ions. $N_{ag} = 14$, $d_{3-4} = 0.3$ nm (panels a, c, and f), and $d_{3-4} = 0$ nm (panels b, d, and g).

which point on surface 3 goes the radius. This result is the consequence of the charges being taken to be discrete. Note that in the spherical capacitor models with a uniformly distributed charge the electrostatic potential does not go beyond the plates. Penetration of Na^+ ions into the layer of potential-determing ions gradually decreases the potential down to zero at $d_{3-4} = 0$ (Figure 7).

In the case of nonspherical micelles, because of an inconsiderable distortion of the charge distribution symmetry under the same conditions, the potential within the micelle is not equal to zero (~0.3 V) and may have different signs at different points.

Effects of Self-Assembling. Consider the influence of the electrostatic interaction of ions in a micelle on the energy of micelle formation. Negative values of E_{CuI} at small values of d_{3-4} and for large aggregation numbers indicate that when the micelles are formed from ions lying at indefinitely large distances from each other the electrostatic energy favors the formation of micelles. However, in nonpolar media, the ions probably exist as ion pairs.[36] Therefore, the formation of micelles of ionic surfactants should be considered to assemble from ion pairs.

As follows from Figures 2 and 5, when the counterions penetrate the layer of the potential-determining ions ($d_{3-4} = 0$), the energy modulus, $|E_{CuI}/N_{ag}|$, is higher than that for isolated ion pairs, $|E_1|$. The value of $|E_1|$ for the Na^+AOT^- pair is equal

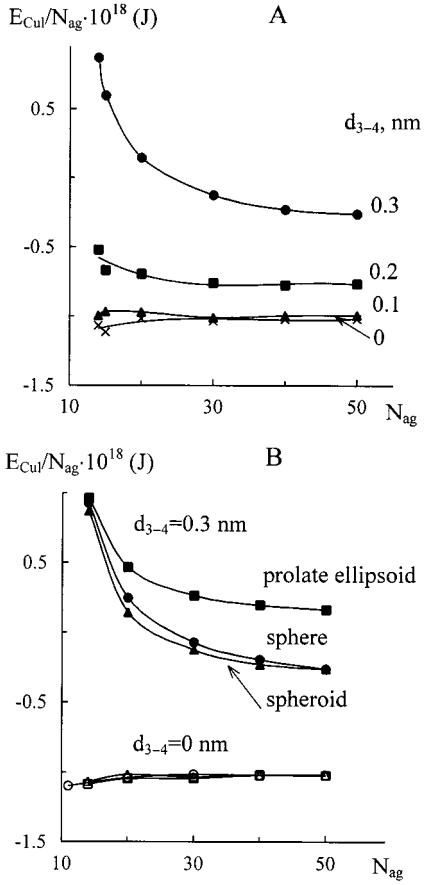

Figure 5. Electrostatic interaction of ions in NaAOT micelles as a function of the numbers of aggregation. (A) Calculation for a spheroid at different values of d_{3-4} (the values are given in the Figure). (B) Calculation for different micellar shapes at $d_{3-4} = 0.3$ nm (solid symbols) and $d_{3-4} = 0$ (open symbols).

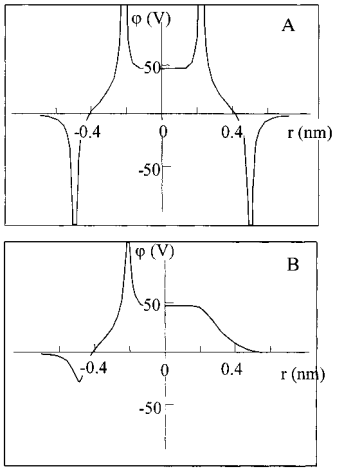

Figure 6. Electrostatic potential distribution along the radius inside the spherical micelle of NaAOT ($N_{ag} = 14$, $d_{3-4} = 0.3$ nm). (A) The radius goes through an arbitrary charge on surface 3. (B) The radius goes through a point equidistant from the nearest charges on surface 3. Corresponding to the point of entry of the radius are the positive values of r. Corresponding to the point of the issue are the negative values of r.

to $\sim 7.7 \times 10^{-19}$ J. This means that under these conditions the electrostatic interactions of ions favors their self-assembling to micelles. It should be noted that this is a new finding and that in principle this result could not be obtained with the models using a uniformly distributed charge.

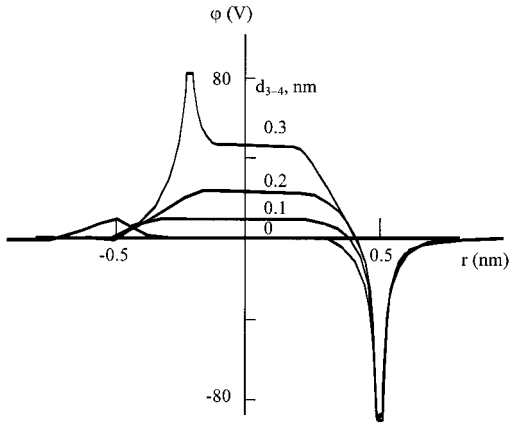

Figure 7. Change of the electrostatic potential along the radius inside a spherical micelle of NaAOT ($N_{ag} = 14$) when Na^+ penetrates the layer of the potential-determining ions. The radius goes through an arbitrary charge on surface 3.

3.3. Structural Parameters of Micelles with Different Counterions. The methodology of optimization developed to calculate the structural parameters of the micelles of NaAOT was used to find the structural characteristics of micelles with other counterions such as Li^+, Cs^+, $Co(H_2O)_6^{2+}$, and La^{3+}. It should be noted that in the case of the $Co(H_2O)_6^{2+}$ ion the effect of the water dipoles on the energy of electrostatic interaction was not taken into account. The complex ion $Co(H_2O)_6^{2+}$ was included because there are no "simple" ions with such a large radius. The structures obtained for this ion rather serve as an illustration. The calculated data for the studied counterions are summarized in Table 1. Shown for each shape are the most "favorable" structures from the point of view of electrostatic interaction ($d_{3-4} = 0$) and the most "unfavorable" (for which d_{3-4} is equal to the sum of the radii of the counterion and the potential-determining ion) structures. The intermediate positions are occupied by the "transitional" structures. So Table 1 reflects the rearrangements in the energy and structure taking place when the counterions penetrate the layer of the potential-determining ions, and this data allows us to estimate the effect of self-assembling for each counterion at low values of the aggregation numbers. We point out once more that for each counterion the regularities of the change in E_{Cul}/N_{ag} with increasing N_{ag} are similar to those obtained for the micelles of NaAOT: the increase in the numbers of aggregation at $d_{3-4} = 0$ leads to an inconsiderable decrease of the modulus of E_{Cul}/N_{ag}. On the contrary, at $d_{3-4} \neq 0$, the modulus increases, but the values of the modulus corresponding to $d_{3-4} = 0$ are not reached even at large values of N_{ag}. Therefore, the structures with $d_{3-4} = 0$ are the most optimal from the point of view of electrostatic interaction.

Table 1 also gives the areas of the inner cavity containing no ions (S_5/N_{ag}). In the right part of the Table are given the hydrodynamic radii of the micelles, r_h, and the overall energies of interaction of ions with each other (E_{++}/N_{ag}, E_{--}/N_{ag}, E_{+-}/N_{ag}). All parameters were calculated for a sphere, a spheroid, and a prolate ellipsoid.

Below is given a brief analysis of the effect of the counterions on the micellar parameters.

3.4. Numbers of Aggregation. Effect of the Size of the Counterions. The numbers of aggregation shown in the first columns of the Tables are the minimal values for the corresponding sizes of the potential-determining ion and the counterion. At smaller values of N_{ag}, the distances between the nearest ions become shorter than the sum of their radii. As the counterion radius increases in the series from Li^+ to Cs^+, there is an increase in the number of aggregation. When the radius of the counterion begins to exceed that of the potential-determining ion considerably (for example, in the case of $Co(H_2O)_6^{2+}$), the growth of the aggregation numbers is more pronounced. For small counterions (Li^+ and Na^+), the penetration of the counterion into the layer of the potential-determining ions has no appreciable influence on the numbers of aggregation, but for Cs^+ and $Co(H_2O)_6^{2+}$ (for a spheroid), this effect is more pronounced and leads to a decrease in N_{ag}.

Dependence on the Charge of the Counterion. The increase of the charge of the counterion from +1 to +3 at an inconsiderable change of the radius (Na^+ and La^{3+}) leads to no substantial changes in the micellar size. This result may be due to the fact that in this case the micellar size is determined by the radius of the potential-determining ion.

A small decrease in the numbers of aggregation for La^{3+} appears to be due to the fact that fewer counterions are required to compensate for the charge of the potential-determining ion.

Micellar Shape. From the data, it follows that for small counterions the change of the micellar shape has no substantial effect on the aggregation numbers, even in the case when the counterions penetrate the layer of the potential-determining ions. In the case of $Co(H_2O)_6^{2+}$, a substantial increase in the numbers of aggregation takes place on going from a sphere to a spheroid. The configuration of a prolate ellipsoid is interesting in that at a constant, small radius further decrease in d_{3-4} becomes impossible; also, the 1-D growth of micelles is impossible, which is due to the fact that for a strongly prolate ellipsoid the parts of the elongated cavity at the micellar ends diminish in volume (although their contribution to the total volume increases) and the counterions cannot penetrate the peripheral part of the micelle because of the steric restrictions.

Density of Micelles. For the micelles containing Li^+, no definite regularities of the micellar density (V_v) behavior with the change of the micellar shape and d_{3-4} could be observed. Minimal values of micellar density were observed both for the maximum value of d_{3-4} (a sphere, a prolate ellipsoid) and the minimum value of this parameter (a sphere). For the micelles containing Na^+, Cs^+, and La^{3+}, on the whole, the micellar density for micelles of different shapes increased as the counterions penetrated the layer of the potential-determining ions. Such a dependence was especially pronounced for a spheroid and a prolate ellipsoid. The densest micelles were formed for the ion with the smallest radius (Li^+). Higher aggregation numbers (when micellar growth was close to 1-D growth) usually led to the formation of looser structures.

Central Voids. The central voids are taken into account in the calculations of the density in the polar part of the micelle. However, for the reasons mentioned above, these voids will be considered separately. In the case of spherical micelles, the area of the central void was the largest for the structures with the smallest values of d_{3-4}. This result is easily understandable. As the counterions leave the center and penetrate the surface layer, a void forms that cannot close in the case of spherical micelles. For the elongated configurations, S_5/N_{ag} goes through a maximum in the case of Li^+ and Na^+, and frequently, it is close to or equal to zero. For Cs^+ and $Co(H_2O)_6^{2+}$, the regularities of the S_5/N_{ag} behavior are very similar for all geometries and coincide with those for the spherical micelles. The voids were the smallest for the micelles with La^{3+} (Table 1, spheroidal micelles).

Partial Coulomb Interactions of Ions of Different Kinds. At the maximum values of d_{3-4}, it is the repulsion that prevails

TABLE 1: Changes of the Structural and Energy Characteristics of Reversed Micelles of AOT with Different Counterions When the Counterion Penetrates the Layer of Potential-Determining Ions

N_{ag}	d_{3-4} (nm)	r_{a3} (nm)	r_{b3} (nm)	V_v (nm^3)	S_5/N_{ag} (nm^2)	E_{cul}/N_{ag} $\times 10^{18}$ (J)	r_h (nm)	E_{++}/N_{ag} $\times 10^{18}$ (J)	E_{--}/N_{ag} $\times 10^{18}$ (J)	E_{+-}/N_{ag} $\times 10^{18}$ (J)
						Li^+				
						sphere				
9	0.00	0.37	0.37	0.052	0.041	−1.255	1.37	1.783	1.778	−4.815
10	0.10	0.41	0.41	0.060	0.054	−1.050	1.41	2.465	1.855	−5.370
9	0.20	0.37	0.37	0.053	0.018	0.069	1.37	3.846	1.776	−5.553
9	0.26	0.37	0.37	0.052	0.004	2.106	1.37	5.911	1.777	−5.582
						spheroid				
11	0.00	0.57	0.20	0.055	0.000	−1.192	1.44	1.985	1.972	−5.149
10	0.10	0.46	0.30	0.058	0.054	−1.106	1.41	2.441	1.878	−5.425
9	0.20	0.38	0.35	0.053	0.017	0.062	1.37	3.844	1.781	−5.563
11	0.26	0.49	0.36	0.066	0.018	0.651	1.44	4.519	1.978	−5.847
						prolate ellipsoid				
9	0.00	0.42	0.35	0.052	0.041	−1.231	1.37	1.796	1.790	−4.841
10	0.10	0.64	0.30	0.053	0.044	−1.090	1.41	2.498	1.924	−5.512
10	0.20	0.49	0.37	0.060	0.027	−0.158	1.41	3.634	1.882	−5.675
10	0.26	0.55	0.34	0.054	0.005	1.531	1.41	5.506	1.967	−5.941
						Na^+				
						sphere				
11	0.00	0.44	0.44	0.064	0.067	−1.098	1.44	1.935	1.928	−4.961
14	0.10	0.54	0.54	0.111	0.103	−0.965	1.54	2.616	2.128	−5.709
12	0.20	0.48	0.48	0.070	0.062	−0.330	1.48	3.440	1.993	−5.763
14	0.30	0.54	0.54	0.082	0.017	0.926	1.54	4.804	2.124	−6.002
						spheroid				
14	0.00	0.72	0.18	0.059	0.000	−1.067	1.54	2.263	2.225	−5.555
14	0.10	0.67	0.28	0.071	0.106	−0.993	1.54	2.683	2.284	−5.960
14	0.20	0.62	0.38	0.079	0.051	−0.522	1.54	3.346	2.246	−6.115
14	0.30	0.58	0.45	0.081	0.017	0.871	1.54	4.809	2.190	−6.128
						prolate ellipsoid				
14	0.00	1.10	0.30	0.059	0.063	−1.085	1.56	2.224	2.146	−5.455
14	0.10	0.90	0.37	0.070	0.088	−1.000	1.54	2.648	2.254	−5.903
14	0.20	0.86	0.39	0.072	0.036	−0.468	1.54	3.459	2.301	−6.229
14	0.30	0.70	0.46	0.080	0.013	0.963	1.54	4.946	2.246	−6.229
						Cs^+				
						sphere				
24	0.00	0.80	0.80	0.119	0.187	−0.902	1.80	2.704	2.703	−6.316
24	0.10	0.80	0.80	0.119	0.145	−0.828	1.80	3.091	2.708	−6.634
24	0.20	0.80	0.80	0.119	0.095	−0.535	1.80	3.603	2.703	−6.841
27	0.37	0.86	0.86	0.132	0.049	0.591	1.86	4.975	2.843	−7.227
						spheroid				
22	0.00	0.83	0.60	0.106	0.172	−0.907	1.75	2.610	2.618	−6.134
24	0.10	0.90	0.60	0.114	0.145	−0.835	1.80	3.114	2.735	−6.683
24	0.20	0.90	0.40	0.072	0.095	−0.544	1.80	3.635	2.751	−6.930
29	0.37	0.92	0.87	0.140	0.057	0.508	1.91	4.969	2.940	−7.402
						prolate ellipsoid				
24	0.00	1.00	0.70	0.115	0.185	−0.902	1.80	2.719	2.716	−6.337
25	0.10	0.90	0.78	0.123	0.152	−0.833	1.82	3.139	2.760	−6.714
25	0.20	0.92	0.77	0.122	0.101	−0.544	1.82	3.641	2.757	−6.942
35	0.37	1.18	0.95	0.164	0.084	0.332	2.03	5.036	3.220	−7.924
						$Co(H_2O)_6^{2+}$				
						sphere				
80	0.13	1.70	1.70	0.504	0.486	−1.707	2.70	9.720	9.562	−20.988
70	0.30	1.57	1.57	0.450	0.319	−1.034	2.57	10.329	8.950	−20.313
80	0.53	1.70	1.70	0.504	0.223	0.824	2.70	12.998	9.505	−21.679
						spheroid				
100	0.13	2.64	0.53	0.275	0.599	−1.753	2.90	11.650	11.775	−25.180
200	0.30	3.93	0.70	0.425	0.684	−1.282	3.80	18.091	17.297	−36.669
200	0.53	3.83	0.93	0.582	0.556	0.306	3.82	20.387	17.797	−37.878
						prolate ellipsoid				
100	0.30	4.08	1.10	0.389	0.323	−1.165	3.02	12.054	10.796	−24.015
						La^{3+}				
						sphere				
9	0.00	0.37	0.37	0.051	0.041	−5.150	1.37	3.248	5.347	−13.746
12	0.10	0.48	0.48	0.072	0.071	−5.132	1.48	5.260	5.997	−16.388
12	0.20	0.48	0.48	0.072	0.027	−4.192	1.48	6.920	5.978	−17.090
12	0.32	0.48	0.48	0.072	0.002	0.359	1.48	11.874	5.966	−17.481
						spheroid				
12	0.00	0.64	0.15	0.051	0.000	−5.352	1.48	4.414	5.967	−15.733
12	0.10	0.62	0.20	0.069	0.000	−5.555	1.48	4.995	6.130	−16.680
12	0.20	0.57	0.30	0.067	0.000	−5.208	1.48	5.651	6.354	−17.213
12	0.32	0.51	0.42	0.071	0.000	−1.130	1.48	10.390	6.007	−17.528
						prolate ellipsoid				
12	0.00	0.87	0.30	0.058	0.057	−5.322	1.48	4.576	6.219	−16.116
12	0.10	0.87	0.30	0.058	0.046	−5.370	1.49	4.930	6.006	−16.306
12	0.20	0.63	0.40	0.069	0.023	−4.657	1.48	6.257	6.194	−17.105
15	0.32	0.90	0.42	0.080	0.000	−1.892	1.57	10.625	7.289	−19.807

TABLE 2: Most Probable Structural Parameters of the AOT Micelles

			shape		r_h (nm)	
counterion	N_{ag}	d_{3-4} (nm)	calcd	exptl	calcd	exptl
Li^+	9	0	sphere		1.37	
Na^+	11	0	sphere	sphere	1.37	1.17[37]
						1.50[38]
						1.64[19]
						1.99[39]
Cs^+	22	0	spheroid		1.75	
$Co(H_2O)_6^{2+}$	100	0.13	spheroid	cylinder	2.9	6.77[a 20]
La^{3+}	12	0.1	spheroid		1.47	

[a] The value of r_h for the spherocylinder calculated from the r_{a1} and r_{b1} data given in ref 20.

in the micelles. The largest contribution to this repulsion is made by the interaction of the counterions (E_{++}) because they lie on the inner surface and undergo a stronger contraction than do the potential-determining ions. With the penetration of the counterions into the layer of the potential-determining ions, the repulsion between the counterions (at a constant value of N_{ag}) decreases because now they are on a surface with a smaller curvature and a larger area. As a result, the attraction of the ions of the opposite sign begins to prevail, and E_{Cul}/N_{ag} changes sign. At values of d_{3-4} of about 0.1 nm (for Li^+, Na^+ and Cs^+), $|E_{Cul}/N_{ag}|$ becomes greater than $|E_1|$ (i.e., the electrostatic interaction of ions favors the formation of micelles (the effect of self-assembling)).

3.5. Optimal Size and Shape of Reversed AOT Micelles. Comparison with Experimental Data. The analysis we performed allows us to draw substantiated conclusions as to the most favored micellar structures for the counterions studied. In doing this, we shall be guided by the following criteria, of which the determining criterion will be the minimal value of E_{Cul}/N_{ag}. Of the structures with similar E_{Cul}/N_{ag} values, preference will be given to micelles with the smallest numbers of aggregation. The next parameters to be taken into consideration are the micellar density and the size of the inner cavity. The main role is assigned to the Coulomb interaction for the following reasons. The work of formation of the largest cavity in the structures that we studied is estimated[23] to be $A = \sigma S_5/N_{ag}$ (σ is the interfacial tension). At $S_5/N_{ag} \approx 1$ nm^2 and $\sigma = 80$ mJ/m^2, the value of $A = 8 \times 10^{-20}$ J indicates that the predominant contribution is made by the Coulomb interaction (at small values of d_{3-4}). At this stage, it is difficult to show that closer packing will be preferred over the structure having a smaller central void (other things being equal). Therefore, structures having the lowest possible (for geometrical reasons) numbers of aggregation whose counterions are closest to the surface of the potential-determining ions are considered to be optimal. The structures meeting the above criteria are shown in Table 2.

From the data in Table 2, it can be concluded that for the cations that do not form complex ions the structures that we obtained are, on the whole, in agreement with experiment. The large scatter of the experimental data for NaAOT, the species that was studied the most, is due to the presence of traces of water in the micellar solutions[19] and to the different polarity of the solvents used. At small aggregation numbers, an accurate determination of micellar shapes from measurements of the hydrodynamic radius is, however, impossible because the large radius exceeds the small radius by no more than 0.2 nm (at small values of d_{3-4}) and the shape of the micelles can be taken to be close to spherical. We note that within this approach the use of the value $r_- = 0.3$ nm[35] gives overestimated values of the numbers of aggregation (21) and the hydrodynamic radius (1.8 nm).

Large differences were obtained for $Co(H_2O)_6^{2+}$. Therefore, structures such as a spherocylinder and a disk should have also been analyzed. Such structures appear to be more preferable because they do not have many of the steric restrictions that exist for the large cations. Besides, the calculations of the electrostatic interaction of $Co(H_2O)_6^{2+}$ did not take into account the possibility of the central atom being screen by water dipoles.

Therefore, this ion cannot be compared with other ions containing no water. At the present stage, the calculations for this ion should be considered to be calculations for a hypothetical two-charge ion of the same radius containing no water. We used this ion in our calculations only to follow the dynamics of the structural rearrangement for large counterions.

4. Conclusions

This work is an attempt to determine structures of micelles by calculating and optimizing the electrostatic interactions of ions and accounting for their sizes. Division of the polar cavity of micelles into different regions allowed us to follow the transition dynamics from one micellar states to another.

The most important result of this study is the finding that at low values of d_{3-4} the electrostatic interaction favors the association of surfactant molecules (the effect of self-assembling).

Note that this result is in quantitative agreement with the data obtained by the method of molecular dynamics:[35] at low water content, the maximum of the Na^+ ion density is on the surface of the potential-determining ions. The treatment of dry micelles of ionic surfactants as ionic crystallites seems to us to be very promising. In this case, the micelle can be considered to be an ionic nanocrystal whose energy is almost entirely determined by the energy of electrostatic interactions. For example, the energy of the crystal lattice of NaCl is almost 90% determined by the Coulomb interactions of ions with each other, the remainder being the Born repulsion and the vibrational energy of the Na^+ and Cl^- ions in crystal lattice nodes.[34] Only the last contribution is temperature-dependent. Therefore, the approximation that $T = 0$ K is not too rough.

It is obvious that the effect of electrostatic interactions in dry micelles is most important in solvents with low dielectric permeabilities. Unfortunately, nonaqueous micelles have received considerably less attention, although such systems may help to solve a series of synthetic tasks that are impossible to solve in the presence of water.[40] Therefore, the results of this work are important because they allow one to determine the probable sizes and shapes of micelles and thus to synthesize nanoclusters with required dimensions.

Acknowledgment. This work is supported by the Russian Foundation for Basic Researches (Grant No. 02-03-32411).

References and Notes

(1) Bansal, V. K.; Shah, D. O. In *Micellization, Solubilization and Microemulsions*; Mittal, K. L., Ed.; Plenum Press: New York, 1977.

(2) Pillai, V.; Kumar, P.; Hou, M. J.; Ayyub, P.; Chah, D. O. *Adv. Colloid Interface Sci.* **1995**, *55*, 241.

(3) Petit, C.; Lixon, P.; Pileni, M. P. *J. Phys. Chem.* **1993**, *97*, 12974.

(4) Magali, B.; Erzy, K.; Per, S. *Colloids Surf.* **1982**, *5*, 209.

(5) Hougi, N.; Taichene, S.; Ganzuo, L. *J. Dispersion Sci. Technol.* **1992**, *13*, 647.

(6) Neuman, R. D.; Zhou, N.-F.; Wu, J.; Jones, M. A.; Gaonkar, A. G.; Park, S. J.; Agrawar, M. L. *Sep. Sci. Technol.* **1990**, *25*, 1655.

(7) Bulavchenko, A. I.; Batishcheva, E. K.; Torgov, V. G. *Sep. Sci. Technol*. **1995**, *30*, 239.
(8) Bulavchenko, A. I.; Podlipskaya, T. Yu.; Batishcheva, E. K.; Torgov, V. G. *J. Phys. Chem. B* **2000**, *104*, 4821.
(9) Pires, M. J.; Aires-Barros, M. R.; Cabral, J. M. S. *Biotechnol. Prog.* **1996**, *12*, 290.
(10) Adach, M.; Harada, M.; Shioi, A.; Sato, V. *J. Phys. Chem*. **1991**, *95*, 7925.
(11) Leodidis, E. B.; Bominarius, A. S.; Hatton, T. A. *J. Phys. Chem*. **1991**, *95*, 5943.
(12) Cavasino, F. P.; Sbriziolo, C.; Liveri, M. L. T. *J. Phys. Chem*. **1998**, *102*, 3143.
(13) Mukherjee, K.; Mukherjee, D. Ch.; Moulik, S. P. *Bull. Chem. Soc. Jpn*. **1997**, *70*, 1245.
(14) Biasutti, M. A.; Sereno, L.; Silver, J. J. *J. Colloid Interface Sci*. **1994**, *164*, 410.
(15) Schmid, G. *Chem. Rev*. **1992**, *92*, 1709.
(16) Schwuger, M. J.; Stickdorn, K.; Schomacker, R. *Chem. Rev*. **1995**, *95*, 849.
(17) Kabie, H. R.; Vora, J. H. *J. Phys. Chem*. **1997**, *101*, 10295.
(18) Caselli, M.; Mangone, A. *Ann. Chim*. **1992**, *82*, 303.
(19) Lekkerkerker, H. N. N.; Kegel, W. K.; Overbeek, J. Th. G. *Ber. Bunsen-Ges. Phys. Chem.* **1996**, *100*, 206.
(20) Eastor, J.; Fragneto, G.; Robinson, B. N.; Towey, T. F.; Heenan, R. R.; Leng, F. I. *J. Chem. Soc., Faraday Trans*. **1992**, *88*, 461.
(21) Leodidis, E. B.; Hatton, T. A. *Langmuir* **1989**, *5*, 741.
(22) Adamson, A. W. *Physical Chemistry of Surfaces*; John Wiley and Sons: New York, 1976.
(23) Rusanov, A. I. *Micelle Formation in Solutions of Surfactants*; Khimiya: Sankt-Peterburg, 1992.
(24) Wong, M.; Thomas, J. K.; Nowak, T. *J. Am. Chem. Soc*. **1977**, *99*, 4730.
(25) Neuman, R. D.; Jones, M. A.; Zhou, N.-F. *Colloids Surf*. **1990**, *46*, 45.
(26) Liu, D.; Ma, J.; Cheng, H.; Zhao, Z. *Chin. J. Appl. Chem*. **1997**, *14*, 51.
(27) Yu, Z.-J.; Zhou, N.-F.; Neuman, R. D. *Langmuir* **1992**, *8*, 1885.
(28) Yu, Z.-J.; Neuman, R. D. *Langmuir* **1994**, *10*, 2553.
(29) Feng, K. I.; Schelly, Z. A. *J. Phys. Chem*. **1995**, *99*, 17207.
(30) Kobson, K. J.; Dennis, E. A. *J. Phys. Chem*. **1977**, *81*, 1075.
(31) Bulavchenko, A. I.; Batishcheva, E. K.; Podlipskaya, T. Yu.; Torgov, V. G. *Colloid J*. **1998**, *60*, 152.
(32) Haadrikman, G.; Daane, G. J. R.; Kerkhof, F. J. M.; Os, N. M. *J. Phys. Chem*. **1992**, *96*, 9061.
(33) Bisal, S.; Bhattachharga, P. K.; Moulik, S. P. *J. Phys. Chem*. **1990**, *94*, 350.
(34) Day, M. C.; Selbin J. *Theoretical Inorganic Chemistry*; Reinhold: New York, 1962.
(35) Faeder, J.; Ladanyi, B. M. *J. Phys. Chem. B* **2000**, *104*, 1033.
(36) Komarov, E. V.; Kopyrin, A. A.; Proyayev, V. V. *Theoretical Foundations of Extraction with Associated Reagents*; Energoizdat: Moscow, 1984.
(37) Fioretto, D.; Freda, M.; Onori, G.; Santucci, A. *J. Phys. Chem*. **1999**, *103*, 8216.
(38) Zulanf, M.; Eicke, H. F. *J. Phys. Chem*. **1979**, *83*, 480.
(39) Lalanne, J. R.; Pouligny, B.; Seln, E. *J. Phys. Chem*. **1983**, *87*, 696.
(40) Wilcoxon, J. P.; Provencio, P. P. *J. Phys. Chem. B* **1999**, *103*, 9809.